

Electronic structure of Pu monochalcogenides and monopnictides

L. Petit^{1,a}, A. Svane¹, W.M. Temmerman², and Z. Szotek²

¹ Institute of Physics and Astronomy, University of Aarhus, 8000 Aarhus C, Denmark

² Daresbury Laboratory, Daresbury, Warrington WA4 4AD, UK

Received 10 August 2001

Abstract. The electronic and magnetic properties of Pu monopnictides and monochalcogenides, PuX (X = N, P, As, Sb, Bi, O, S, Se, Te, Po), are studied using the *ab initio* self-interaction-corrected local spin-density approximation. This approach allows for an integer number of f -states to be localized, while the remaining f -electron degrees of freedom are available for band formation. By varying the relative proportions of localized and delocalized f -states, the energetically most favourable (groundstate) configuration can be established. We show that the experimental data can be interpreted in terms of the coexistence of both localized and delocalized f -states.

PACS. 71.27.+a Strongly correlated electron systems; heavy fermions – 71.28.+d Narrow-band systems; intermediate-valence solids – 71.15.Nc Total energy and cohesive energy calculations

1 Introduction

The quantum-mechanical understanding of the physics of elemental Pu as well as Pu compounds presents a great challenge due to the intricate nature of the Pu $5f$ electrons. Pu is situated at the borderline of the localized-delocalized f -electron transition that occurs in the actinides series. The phase diagram of Pu metal is extremely rich, reflecting the highly susceptible $5f$ electron manifold, and includes the low-symmetry α -Pu groundstate as well as the large-volume fcc phase of δ -Pu [1].

It is well established that neither the local spin density (LSD) [2] nor the semi-local generalized gradient (GGA) [3] approximations to density functional theory are able to describe the electronic and magnetic properties of all the phases of metallic Pu [4, 5]. For a realistic description of the electronic structure of Pu, both correlations and valency fluctuations have to be considered at a level beyond what is offered by the one-electron band picture. Several methods have been proposed that use a localized partially filled f -shell as the starting point for calculations. The most well known extensions of LSD, capable of describing electron localization, include the self-interaction corrected (SIC)-LSD [6, 7], LDA+U [8], and orbital polarization (OP) methods [9]. All of these methods have been applied to Pu [10–12] proving that important aspects of the Pu problem are accounted for by f -electron localization, although f -electron fluctuations are significant [13].

The partially band-like and partially atomic-like character of the f electrons seems to persist in Pu compounds, of which the monochalcogenides and monopnictides are

the most widely studied. Measurements for PuS, PuSe, and PuTe show a semiconductor-like decrease of the electrical resistivity with increasing temperature [14]. This would indicate that the Fermi energy is situated in a small gap in the density of states (DOS). However, the measured magnetic susceptibilities are temperature independent [15] and relatively high which, if interpreted as Pauli paramagnetism, means that we have a relatively large DOS at the Fermi energy. Assuming localized f electrons, one has a choice between the f^6 configuration, which would explain the absence of magnetic moment, but the corresponding divalent Pu ion would lead to a much too large lattice constant, and the f^5 configuration, which gives an acceptable lattice constant but is magnetic, in contradiction with experiment. Different band-theory models have been invoked, which respectively describe the Pu monochalcogenides as either relativistic semiconductors [16] or semi-metals [17, 18]. In the relativistic band structure calculations [16], the semiconductor gap is identified with the gap that appears between the $j = 5/2$ and $j = 7/2$ subbands, due to the spin-orbit interaction. The corresponding calculated lattice constants are in good agreement with experiment. However, the f electrons have been treated as band states, *i.e.*, the correlations that tend to localize the electrons on their own sites have been ignored although even in UTe, where f electrons are considerably more delocalized than in PuTe, one already observes Kondo-like behaviour [19]. To account for the experimental data, a picture has been proposed [14, 20] where the semiconducting gap results from the hybridization of a very narrow f band with the conduction electron bands.

For the Pu monopnictides, the effective moments, derived from high temperature Curie-Weiss-like behavior of

^a e-mail: lpetit@ifa.au.dk

the susceptibility [21], are relatively close to the value of $1.24 \mu_B$, expected for an f^5 ion, corresponding to trivalent Pu ions. The ordered magnetic moments [21] are significantly smaller than the measured effective moments, which to some degree can be explained in terms of crystal field effects. Although experiments point towards f -electron localization in Pu pnictides, they also indicate that the localization is not complete. For example, Lander *et al.* [23] have shown that the crystal field can not explain the reduction of the ordered magnetic moment in PuP. There has been some controversy in the literature as to whether a temperature independent component of the susceptibility exists for PuP [24,25]. Even in PuSb, where X-ray photoemission studies indicate clearly localized f electrons [26], the resistivity measurements show a semi-metallic Kondo-like behaviour [27]. Magnetization experiments find a very strong anisotropy in all Pu pnictides [28], with the magnetic moments oriented along the [100] direction. Results from neutron scattering experiments [22] support the interpretation by Cooper *et al.* [29], according to which the moderate f -electron delocalization, rather than the crystal field, is responsible for the reduction of the ordered moment and strong magnetic anisotropy in the Pu monopnictides.

In the present work SIC-LSD calculations of Pu monopnictides and monochalcogenides are presented. It will be demonstrated that this scheme provides a consistent picture of these Pu compounds. As regards the f -electrons, the SIC-LSD [7] scenario can be viewed as an interpolation between the fully localized and fully itinerant pictures. The fully itinerant picture can be implemented in band-theory by simply letting the f -states hybridize into the valence bands, which will lead to a relatively narrow set of f -bands around the Fermi level (Fig. 1b). The fully localized picture can be implemented by occupying a fixed number of f -states as core states and projecting out all f -degrees of freedom from the valence bands. Thus, the f -states are represented by delta function peaks in the density of states diagram, as in Figure 1a. This approach has been successfully applied to rare earth compounds [30]. The $5f$ -electrons in the actinides are less inert and can play quite a significant role in bonding, especially in the early actinide compounds. At the same time the $5f$ -electrons are correlated, and increasingly so for the heavier actinides. The SIC-LSD approach effectively puts an integer number of states (in practice of f -character) into the core, but places no restrictions on the remaining f -degrees of freedom, which are available for band formation. Thus, a picture as displayed in Figure 1c emerges [31]. It introduces two kinds of f -electrons [32], the integer number of localized states and a non-integer number of hybridized band- f electrons, determined by the self-consistent position of the Fermi level. The localized electrons acquire core-like characteristics by correcting the LSD total energy functional for their spurious self-interaction [6]

$$E^{\text{SIC}} = E^{\text{LSD}} - \sum_{\alpha}^{\text{occ.}} \delta_{\alpha}^{\text{SIC}}. \quad (1)$$

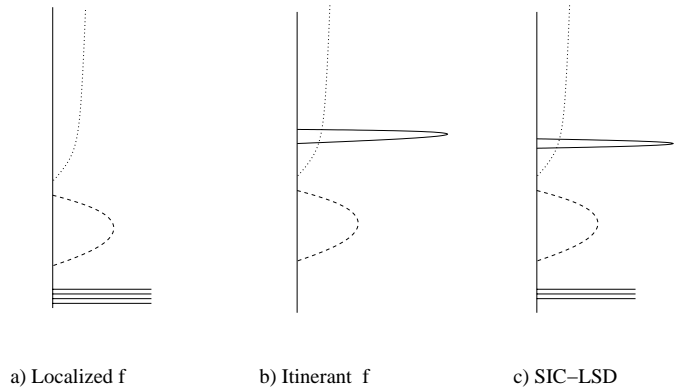


Fig. 1. Schematic representation of the density of states for the Pu monopnictides and monochalcogenides. a) LSD calculation with all f electrons treated as inert core electrons, b) LSD calculation with all f electrons treated as band states, and c) SIC-LSD calculation with both localized and delocalized f states. The dashed line represents the ligand p -band, while the broad actinide d -band is given by the dotted line, and f -states are shown with full line.

The self-interaction correction $\delta_{\alpha}^{\text{SIC}}$ for a state α is given as the sum of the Hartree and exchange-correlation energies

$$\delta_{\alpha}^{\text{SIC}} = U[n_{\alpha}] + E_{\text{xc}}^{\text{LSD}}[n_{\alpha}]. \quad (2)$$

This correction vanishes for an itinerant state, and therefore the SIC-LSD functional for such a state coincides with the conventional LSD functional. The rationale behind the functional in equation (1) is that for a delocalized electron the interaction with a given atom is well described by the mean-field LSD potential. However, for a localized electron, due to a large Wigner delay time, this potential will be corrected for the fact that other electrons on that atom rearrange in response to the presence of the localized electron.

The number of localized f -electrons leads to a definition of valency of the actinide ions, given as the integer number of electrons available for band formation, *i.e.*

$$N_{\text{val}} = Z - N_{\text{core}} - N_{\text{SIC}},$$

where Z ($= 94$) is the atomic number of Pu, N_{core} is the number of core (and semi-core) electrons (which for Pu is 86), and N_{SIC} is the number of localized f -electrons on the Pu sites. Due to a substantial f -character of the bands, this valency is not the same as that determined by the total f -electron count, which includes both localized and itinerant f -electrons, and which is usually non-integral. By assuming different f^n configurations of localized electrons, various valency states can be realized and studied in detail. Thus, *e.g.* a trivalent Pu^{3+} configuration is obtained by localizing five electrons on the atoms (f^5 configuration). To benefit from the self-interaction correction, an electron state needs to spatially localize, which costs band formation energy due to loss of hybridization. Whether this is favorable depends on the relative magnitudes of the hybridization energy and the self-interaction correction energy. For a given f^n configuration, the minimum

in the total energy as a function of lattice parameter determines the theoretical equilibrium lattice constant. By comparing the total energy minima for different f^n configurations, the global groundstate configuration and lattice constant can be determined.

When applied to Pu metal [10] in the fcc structure the SIC-LSD method leads to a trivalent groundstate with an equilibrium lattice constant, which is about 10% too large as compared to the experimental lattice constant of δ -Pu. Hence, localization is overestimated in elemental Pu, which is due to the neglect of Pu spin fluctuations at metallic densities [33]. In the Pu monochalcogenides and monopnictides, due to a considerably larger separation between the Pu atoms, the f electrons are expected to be more localized, which leads us to believe that applying SIC-LSD to these compounds will result in a more adequate description of their electronic structure. The SIC-LSD has recently been successfully applied to the similar Am compounds [34].

2 Results

The SIC-LSD scheme has been implemented [7] within the tight-binding linear-muffin-tin orbitals (TB-LMTO) method [35]. The Pu semi-core $6s$ and $6p$ states have been described with a separate energy panel. The k -space sampling has been performed with 95 k -points in the irreducible part of the Brillouin zone. Spin-orbit coupling has been fully included in the self-consistency cycles. For simplicity, we have assumed ferromagnetic arrangement of the magnetic moments. In selecting the f^n configuration, the Hund's rules have been followed by aligning spins and maximizing the orbital moment in the direction opposite to the spins. During the iterations towards self-consistency the localized states have been allowed to relax, although generally they do not change much.

Before presenting the SIC-LSD results, let us briefly discuss the expected complication of the underlying physical situation. The f - f and f - d overlaps between neighbouring Pu atoms, and the f - p overlap between Pu and pnictide/chalcogenide atoms, will clearly favor band formation. On the other hand, the strong intra-atomic correlations among f -electrons will tend to localize them on their own sites. The f - p hybridization is considerable due to the large extent of the ligand p orbitals. Consequently, the ligand p -bands will include tails of Pu f character. This hybridization is well described within LSD, as the p -bands are broad and correlations relatively unimportant. The f - d and f - f overlaps between neighbouring Pu atoms depend critically on the Pu-Pu separation and the spatial extent of the f orbitals. This can give rise to three possible scenarios that need to be considered. When the overlap is very small there will be no significant hybridization energy, and it will be favourable to localize the f electrons, gaining the self-interaction correction energy. For a considerable overlap, the f -states will form bands, and correlation effects will be relatively unimportant. In the third scenario, the hybridization energy and self-interaction correction energy are of similar

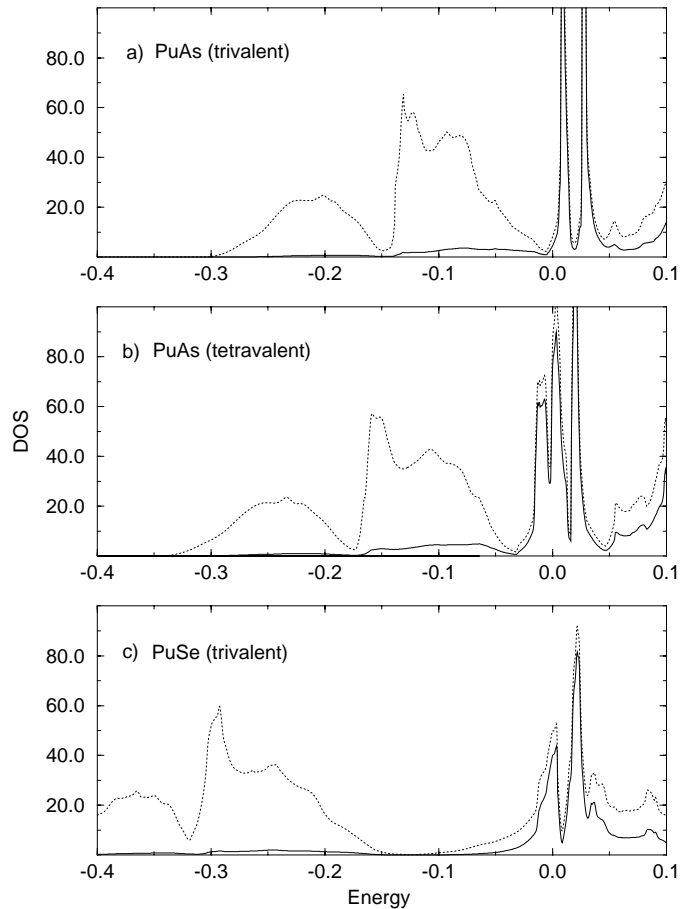


Fig. 2. Density of states, in states per Rydberg and formula unit, for a) PuAs in the trivalent Pu configuration, b) PuAs in the tetravalent Pu configuration and c) PuSe in the trivalent Pu configuration. The solid and dotted lines represent the f projected- and total densities of states, respectively. The energies are given in Ry, with the Fermi energy at zero.

importance, and the f -states are on the verge of being localized. In this case narrow bands will be formed, and correlations in the band description will be relatively important. The proper solution to this problem would require taking into account many-body effects that lie beyond the scope of the LSD method. Regarding the first two scenarios, they are embedded within the SIC-LSD description: The n SIC localized states cannot participate in hybridization, but the delocalized f -electrons, for which the electron-electron correlations are considered relatively unimportant, can be described within the scope of LSD.

2.1 Pu monopnictides

In Figures 2a and 2b the density of states of PuAs for respectively the trivalent and tetravalent groundstate configurations, calculated within SIC-LSD, are shown. In the trivalent SIC-LSD calculation, five f -electrons on each Pu atom are self-interaction corrected. The corresponding δ -function like features in the DOS, occurring well below the

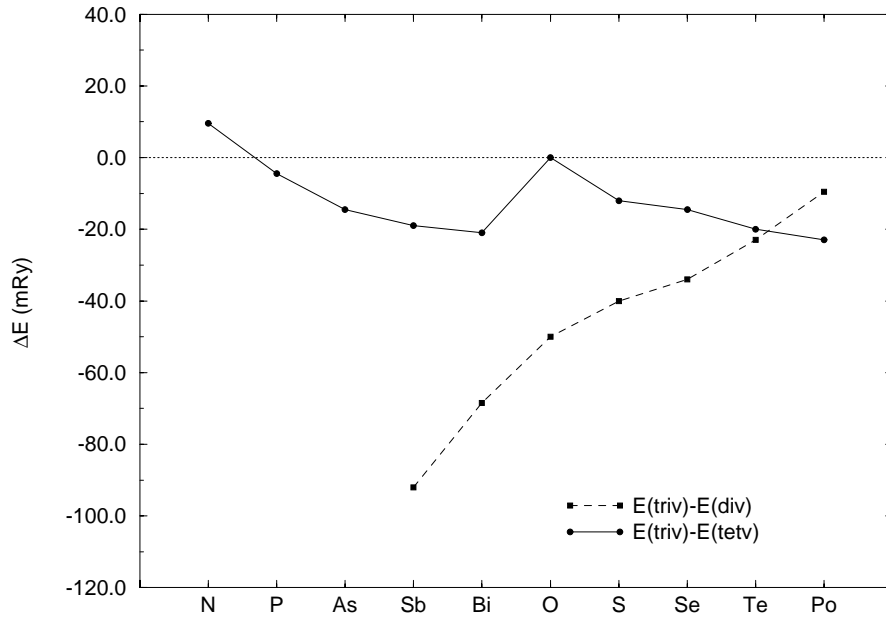


Fig. 3. The energy differences (in mRy) between the trivalent and divalent (dashed line) and the trivalent and tetravalent (full line) Pu configurations in the Pu mononpnictides and monochalcogenides.

valence bands, are not included in the figures. The remaining f -states are allowed to delocalize, which on one hand leads to hybridization with the anion- p band, and on the other gives rise to narrow f peaks (solid line), just above the Fermi level. These f peaks are broadened due to a considerable f - d hybridization. In the pnictide atoms, the valence p states are only half-filled, and therefore, when forming a binary compound, the corresponding p -band can accommodate three electrons from the Pu atom through hybridization and charge transfer. Hence, in the trivalent configuration the three valence electrons fill up the broad pnictide p band. The sharp f - d peaks, originating from the delocalized f -degrees of freedom, lie just above the Fermi level. In the tetravalent configuration there will be one more f - d peak and one more band electron, which will fill up the lowest lying f - d peak, as seen in Figure 2b. In effect, the difference in total f -electron occupation between the trivalent and divalent scenarios will be much smaller than one.

From the calculations of the total energies for several different localized f^n configurations the trivalent configuration is found to be more stable than the divalent and tetravalent configurations for all the pnictides except PuN. This is illustrated in Figure 3 where the respective differences in total energy are plotted. Compared to the trivalent configuration, the divalent configuration is clearly unfavourable for all pnictides. The tetravalent configuration becomes competitive only for the lighter ligands. In PuN the sign of the energy difference changes, and for this compound the calculations show that the pentavalent configuration (f^3) wins over the tetravalent configuration, but further f -electron delocalization is not favourable.

In a purely localized f -electron picture the effective magnetic moment, μ_{eff} , for a given configuration may be calculated from the total angular momentum J and the associated Landé g -factor, g_L . This leads to $\mu_{\text{eff}} = 0.84 \mu_B$ ($J = 2.5$) and $\mu_{\text{eff}} = 2.68 \mu_B$ ($J = 4$), for Pu^{3+} and Pu^{4+} , respectively. Compared to experimental values [21] of approximately $\mu_{\text{eff}} \simeq 1.0 \mu_B$ for the Pu pnictides, this would seem to indicate the presence of Pu^{3+} ions with five localized f -electrons, in good agreement with the predicted trivalent groundstate configuration. Nevertheless, in the SIC-LSD picture, which allows for both localized and delocalized f electrons, these experimental findings do not disagree with the tetravalent scenario either. The reason is that a narrow f -dominated band (as that occupied in Fig. 2b) may carry both a spin and an orbital moment, contributing to the Curie-Weiss-like susceptibility [36]. In this respect the calculated total angular momentum will, in both the trivalent and tetravalent configurations, approach the ionic Pu^{3+} value $J = 2.5$. The calculated total angular momenta, J , and the effective moments of Pu compounds are displayed in Table 1. The experimental effective moments are determined by the high-temperature behavior of the magnetic susceptibility, which is proportional to $\mu_{\text{eff}}^2 = g_L^2 J(J+1)$. Lacking any appropriate theory for the coupling of band f -states and localized f -states, the Landé g -factor was taken to be $g_L = 0.286$, as appropriate for an f^5 ion in LS coupling. The calculated total angular momentum is seen to decrease steadily across the Pu pnictides (from PuP). This is due to the combined effect of decreasing orbital moment and increasing spin moment, which reflect that the total f -occupancy increases, from $n_f = 5.08$ in PuP to $n_f = 5.26$ in PuBi (trivalent Pu configuration). The effective

Table 1. Total angular momentum, $J = L - S$ in units of \hbar , and effective magnetic moment, μ_{eff} in units of μ_{B} , calculated for respectively the pentavalent, tetravalent, and trivalent Pu configurations. The experimental effective moments from reference [13] are quoted for comparison.

| Compound | f^3 - Pu(5+) | | f^4 - Pu(4+) | | f^5 - Pu(3+) | | Exp. |
|----------|----------------|--------------------|----------------|--------------------|----------------|--------------------|--------------------|
| | J | μ_{eff} | J | μ_{eff} | J | μ_{eff} | μ_{eff} |
| PuN | 1.67 | 0.60 | - | - | - | - | 1.1 |
| PuP | 1.94 | 0.68 | 2.14 | 0.74 | 2.29 | 0.78 | 0.97 |
| PuAs | - | - | 1.81 | 0.64 | 2.11 | 0.73 | 1.0 |
| PuSb | - | - | 1.74 | 0.62 | 2.06 | 0.72 | 1.0 |
| PuBi | - | - | 1.51 | 0.56 | 1.86 | 0.66 | 0.8 |
| PuO | 1.17 | 0.46 | 1.89 | 0.66 | 1.68 | 0.61 | - |
| PuS | - | - | 1.17 | 0.46 | 1.42 | 0.53 | 0 |
| PuSe | - | - | 0.98 | 0.40 | 1.24 | 0.48 | 0 |
| PuTe | - | - | 0.86 | 0.36 | 1.20 | 0.46 | 0 |
| PuPo | - | - | - | - | 0.89 | 0.37 | - |

moment decreases similarly across the pnictide series, in accord with the experimental trend, although the calculated value is somewhat too small. The moments are seen to be only slightly reduced in the tetravalent and pentavalent calculations, as compared to the trivalent case. Thus, the tetravalent configuration could explain both the measured effective moment, and those measurements that suggest a moderate delocalization, especially in the lighter pnictides. However, the calculated total energy shows that this trend towards weak delocalization of the Pu^{3+} f -shell is not strong enough for the tetravalent configuration to become favourable (except for PuN). From the comparison of the calculated lattice constants to the experimental values, presented in Table 2, a different picture emerges. Here a valency transition is predicted. For PuSb and PuBi, the experimental lattice constants are in good agreement with the calculated trivalent value, but for PuP and PuAs the tetravalent values give a better agreement. Based on the fact that the overlap between orbitals on neighbouring Pu sites is larger in the light pnictide compounds, with small lattice constants, than in heavier pnictides, this trend is in line with expectations. Thus, the present calculations lead to contradicting results, as the total energy differences point towards trivalency in PuP and PuAs, while the lattice constants favor the tetravalent scenario. One possible explanation of this discrepancy is that at this point of transition from localized to delocalized f -electron behavior, the simple tetravalent SIC-LSD picture is too restricted, and a scenario of the f -shell destabilization, where all f electrons can participate in the delocalization process, is more appropriate. Hence, the band-formation energy gained in the tetravalent calculation would be underestimated. Another possible explanation relates to the tetrad effect [37], which is of purely atomic origin. Due to different coupling schemes for the competing f^4 and f^5 configurations, in its ground state multiplet, the former has lower energy, with respect to the average f^4 energy (the grand bary center), than the f^5 groundstate multiplet, with respect to the average f^5 energy. Taking this into account within SIC-LSD would result in adding a

Table 2. The calculated lattice constants (in Å) of Pu monopnictides and monochalcogenides, for different Pu configurations, in comparison with experimental values [41].

| Compound | a_0 (II) | a_0 (III) | a_0 (IV) | a_0 (V) | a_0 (exp) |
|----------|------------|-------------|------------|-----------|-------------|
| PuN | - | 5.13 | 5.05 | 4.94 | 4.905 |
| PuP | - | 5.76 | 5.65 | 5.59 | 5.550 |
| PuAs | - | 5.95 | 5.87 | - | 5.858 |
| PuSb | 6.50 | 6.24 | 6.18 | - | 6.241 |
| PuBi | 6.46 | 6.32 | 6.30 | - | 6.358 |
| PuO | 5.22 | 5.12 | 5.00 | 4.93 | 4.960 |
| PuS | 5.76 | 5.65 | 5.54 | - | 5.541 |
| PuSe | 5.99 | 5.76 | 5.72 | - | 5.793 |
| PuTe | 6.42 | 6.24 | 6.20 | - | 6.183 |
| PuPo | 6.68 | 6.53 | 6.50 | - | - |

negative correction to the energy of the tetravalent configuration. It is, however, difficult to estimate the size of the tetrad effect in the solid state environment, although approximations have been introduced [9]. Compared to the effect of the f shell destabilization, the tetrad correction should not be strongly volume dependent, which could then explain the good agreement between the calculated tetravalent lattice constants and the experimental values for PuAs and PuP. Note that the PuN lattice constant for a pentavalent Pu ion is quite close to the experimental value, which is somewhat reassuring for the SIC-LSD approach. There exists no tetrad correction between the penta- and tetravalent Pu configurations.

As mentioned earlier, the hybridized f - d bands are only well described in the SIC-LSD, if correlations are unimportant. An exact treatment implies the description of the interaction between the localized f -state and the conduction band electrons, and the concept of weak hybridization, as suggested by Cooper *et al.* [29]. This theory, based on the Coqblin-Schrieffer model [38], predicts that

weak hybridization between a localized state and conduction electron bands results in anisotropic exchange forces. It is generally believed that the magnetic anisotropy in Ce and U compounds is due to this effect [21,29]. Because of weak hybridization it only concerns those f levels that are degenerate with the conduction band states at the Fermi energy. In the SIC-LSD description, the f - d band states represent the uncorrelated limit of the localized f -state interacting with the conduction band states, and the hybridization is weak in the sense that the SIC corrected states are not available for hybridization. Consequently, anisotropic exchange will not occur, if the f - d band states are largely unoccupied, and in those Pu pnictides where the anisotropic exchange forces are strong, we also expect the tetravalent SIC-LSD configuration to be energetically more favorable. Using the Anderson model lattice Hamiltonian, with parameters derived from the first principles theory, Wills and Cooper have performed calculations for PuAs, PuSb, PuBi, and PuTe [39]. For pnictides they have found that hybridization in PuAs is stronger than in PuSb and PuBi. This finding can be correlated with an increased localization in the heavier pnictides, and is in good agreement with the corresponding increasing trend towards trivalency observed in the present calculations from PuAs to PuSb.

2.2 Pu monochalcogenides

For Pu chalcogenides, the SIC-LSD calculations again show a discrepancy between the total energies (Fig. 3), which predict a trivalent groundstate for all chalcogenides except PuO, and the equilibrium lattice constants (Tab. 2), with the experimental lattice constants of PuO and PuS being best reproduced by the tetravalent calculations. Taking the tetrad effect into consideration, a picture similar to that of the pnictides emerges, with the early chalcogenides (PuO and PuS) being more delocalized, as in the tetravalent description, whilst the heavier chalcogenides (PuSe and PuTe) are trivalent.

Despite obvious similarities between pnictides and chalcogenides, their electronic structures differ considerably. Most noticeable are differences in their magnetic properties [40], where susceptibility measurements at high temperature indicate almost complete Curie-Weiss behaviour for the pnictides, whilst in chalcogenides the susceptibilities between 50 K and 300 K are almost temperature independent. The strongly anisotropic ordered magnetic structures, observed at low temperatures in the Pu pnictides, do not occur in the paramagnetic Pu chalcogenides. The present SIC-LSD result for the trivalent configuration is consistent with these experimental findings. To see this, consider the DOS of PuAs and PuSe shown in Figures 2a and 2c. Both figures refer to the trivalent configuration, *i.e.*, with five f electrons localized. One can see that in PuAs, the Fermi energy lies above the broad p band, but below the narrow f peaks which correspond to the two itinerant majority f electrons. Hence, the DOS at the Fermi energy is low. In contrast, PuSe

has a large DOS at the Fermi energy. Thus, in the trivalent scenario, band- f electron hybridization is significantly larger in PuSe than in PuAs. This is also true in the model Hamiltonian calculations of Wills and Cooper [39].

In terms of Pauli paramagnetism, the calculated densities of states for PuSb and PuSe, in the trivalent configuration, reproduce qualitatively the experimentally observed susceptibilities. The vanishing magnetic moment in PuSe can be related to the “*de facto*” f^6 configuration, resulting from adding an almost filled spin-polarized f peak to the five SIC localized f electrons. This is in stark contrast to PuAs, where Pu donates three valence electrons into the ligand p band. This puts Pu in an essentially f^5 configuration, with a measurable magnetic moment. The calculated moments of Table 1 are $0.72 \mu_B$ and $0.48 \mu_B$ for PuSb and PuSe, respectively. Quantitatively, the calculated J values for the Pu chalcogenides are reduced with respect to the corresponding values in the pnictides, as can be seen from Table 1, but they are not zero as it would be the case for an f^6 configuration. Only the divalent configuration has $J = 0$, but energetically this configuration is not favored, and the corresponding equilibrium lattice constant is also too large. In a photoelectron spectroscopy study [26], the electronic structures of PuSb and PuSe have been compared, and it was found that f electrons are localized in PuSb, whereas in PuSe signatures of both localized and delocalized $5f$ -electrons have been identified, with the delocalized features appearing as an f -spectral weight at the Fermi energy. Although no definite interpretation has been proposed for these spectroscopic data, the main features are well explained in terms of the SIC-LSD scenario with two kinds of f -electrons: The localized signal would be related to the localized f^5 self-interaction corrected states, whilst the signal at the Fermi energy would originate from the delocalized f electron of trivalent PuSe.

The present SIC-LSD calculations for Pu chalcogenides do not reproduce the small energy gap or pseudogap at the Fermi energy, which is expected based on the analysis of the experimental data of Wachter *et al.* [20]. These authors have concluded that PuTe is an intermediate-valent compound with a gap arising from hybridization of an extremely narrow f band with a broad d band. An extremely narrow f band, which contains all the f -electrons and thus is close to half-filling, is difficult to imagine, since one would expect the intra-atomic exchange and spin-orbit interactions to split the different one-electron f -levels. A hybridization gap would still be possible in the trivalent SIC-LSD scenario, involving the single delocalized f state and the d band. Since the remaining significant correlations in this band are ignored, the effect of the f - d hybridization is overestimated. This would explain why, instead of a hybridization gap, a broadening of the f band is observed in the calculations. By artificially diminishing the f - d hybridization matrix elements in the calculation, we have indeed obtained a pseudogap, but a more complete many-body treatment would be required for a true *ab initio* description of this feature. Oppeneer *et al.* [18] have performed a relativistic non-spin-polarized calculation for PuTe, taking into

account hybridization between $f_{5/2}$ and d states. Their calculation has resulted in a lower f occupancy than six, which again can be interpreted in terms of intermediate valency.

3 Discussion

There are several points regarding the SIC-LSD approach that need to be stressed here. The concept of valency in the SIC-LSD framework refers to the induced destabilization of the f -shell in the solid state environment, rather than to a change of character from f to non- f type. Within the SIC-LSD scheme the valency shifts happen in steps, since the number of localized f -electrons is always integral. The prevailing picture is that, when going from Am to Np, the f -electron delocalization happens as a consequence of a continuous destabilization of the entire f -shell, *i.e.*, all f electrons get equally delocalized, through an increased overlap between the f states and the orbitals on the neighbouring sites. However, in the SIC-LSD approach, the f -electron delocalization is more common than is usually considered to be the case. This is mostly due to the slightly different definitions of delocalization and valency in the SIC-LSD method. A transition from tetravalent to trivalent state in the SIC-LSD picture reflects just a localization of a previously moderately delocalized (*i.e.*, narrow band) f -electron, which is completely different and energetically less costly than promoting an s or d electron to an f shell.

In the SIC-LSD calculations, each single f electron can be treated as either localized or delocalized, which introduces an extra degree of freedom into the electronic structure calculations. As already discussed, in this framework, a tetravalent configuration can explain the experimental magnetic data as well as the trivalent localized state would do. The question remains, however, whether the stepwise delocalization of the f electrons in the SIC-LSD approach reflects the physical situation in the Pu pnictides and chalcogenides, or whether it only provides a better average description of the moderate delocalization of the entire f electron manifold. No clear-cut experimental evidence for a stepwise f -shell delocalization exists. However, as discussed in the previous sections, many experimental data can be explained along these lines. The transition from localized to moderately delocalized f -electron behavior, which is implicated by the magnetic properties of Pu compounds, *e.g.* from the heavier pnictides to the lighter ones, can be explained in terms of a trivalent to tetravalent transition in the SIC-LSD approach. The measured magnetic anisotropies can be, to a certain degree, correlated with the existence of a significant f - d hybridization in the tetravalent pnictides and trivalent or tetravalent chalcogenides. The coexistence of both localized and delocalized f electrons provides a straightforward explanation of the observed features in the photoemission experiments on PuSe.

It appears that the chalcogenides are less well described within the SIC-LSD method than the pnictides. The same was also observed when applying the method

to the Am compounds [34]. It was shown that the main problem of the SIC-LSD approach lay in describing the interaction of the localized f with the band d electrons. A moderate delocalization of the entire f -manifold would consequently lead to similar problems in the description of both pnictides and chalcogenides. If, on the other hand, all the f electrons are assumed to remain localized, the SIC-LSD calculations should again give equally good results for both the pnictides and chalcogenides. In the SIC-LSD approach only the outer shell f -levels are available for f - d hybridization, whilst the remaining f -levels stay localized, and it can be argued that in the chalcogenides f - d hybridization is relatively more important due to the fact that the p band contains one Pu valence electron less. Since correlations are neglected when describing the f - d bands, a less satisfactory agreement with experiment is therefore to be expected for the chalcogenide compounds.

From the trends in energy differences, displayed in Figure 3, it is clear that in the pnictides, the divalent configuration is never favoured. To switch to this configuration from a trivalent configuration would involve the transfer of an electron from the top of the pnictide p -band to a localized f -state. In contrast, the different electronic structure of the chalcogenides with trivalent Pu configuration makes localization of an additional f -electron to be less costly, as essentially no charge transfer is needed. In the heavier Pu compounds (PuSb, PuBi, PuTe and PuPo), delocalizing one additional f -electron, with respect to the trivalent scenario, costs the SIC localization energy, while no compensating hybridization energy is gained. A smaller energy difference, $E(\text{triv})-E(\text{tetv})$, in the light Pu compounds shows that hybridization energy gain begins to outweigh the loss in localization energy.

4 Conclusions

Calculations of the electronic structures of monopnictides and monochalcogenides of Pu, based upon the SIC-LSD approach, have been presented. The Pu f -electron manifold has been described in a mixed picture of localized and delocalized states. The self-interaction correction in this approach provides a localization energy for each f -electron, which competes with hybridization energy, gained by a delocalized f -electron. The calculations have shown that the trivalent Pu configuration is favored in most compounds, but a valency transition has been encountered. In the lightest Pu compounds, the increasing destabilization of the localized f -shell has manifested itself in the fact that the tetravalent, and for PuN even the pentavalent, Pu configuration has become the groundstate configuration. In these cases one or more f -electrons have occupied narrow bands situated below the Fermi energy.

A detailed comparison with experimental data has been presented for the equilibrium lattice constants. In general, they are well reproduced, demonstrating that the bonding energies are well described by the SIC-LSD method. However, several aspects of the magnetic properties of the Pu compounds have not been adequately described, most notably the ordered moment reduction

and anisotropic exchange interactions. These phenomena are governed by the low-energy correlation effects, such as Kondo screening and spin fluctuations, which are not included in the mean-field description of the SIC-LSD method.

This work has been partially funded by the Training and Mobility Network on ‘Electronic Structure Calculation of Materials Properties and Processes for Industry and Basic Sciences’ (contract:FMRX-CT98-0178).

References

1. J. Donohue, *The Structure of the Elements* (Wiley, New York, 1974).
2. R.O. Jones, O. Gunnarsson, *Rev. Mod. Phys.* **61**, 689 (1989).
3. J.P. Perdew, J.A. Chevary, S.H. Vosko, K.A. Jackson, M.R., Pederson, D.J. Singh, C. Fiolhais, *Phys. Rev. B* **46**, 6671 (1992).
4. P. Soderlind, O. Eriksson, B. Johansson, J.M. Wills, *Phys. Rev. B* **50**, 7291 (1994).
5. M.D. Jones, J.C. Boettger, R.C. Albers, D.J. Singh, *Phys. Rev. B* **61**, 4644 (2000).
6. A. Zunger, J.P. Perdew, G.L. Oliver, *Solid State Commun.* **34**, 933 (1980); J.P. Perdew, A. Zunger, *Phys. Rev. B* **23**, 5048 (1981).
7. W.M. Temmerman, A. Svane, Z. Szotek, H. Winter, in *Electronic Density Functional Theory: Recent Progress and New Directions*, edited by J.F. Dobson, G. Vignale, M.P. Das (Plenum, New York, 1998), p. 327.
8. V.I. Anisimov, J. Zaanen, O.K. Andersen, *Phys. Rev. B* **44**, 943 (1991).
9. M.S.S. Brooks, *Physica B* **130**, 6 (1985); O. Eriksson, M.S.S. Brooks, B. Johansson, *Phys. Rev. B* **41**, 7311 (1990).
10. L. Petit, A. Svane, W.M. Temmerman, Z. Szotek, *Sol. State Commun.* **116**, 379 (2000).
11. O. Eriksson, J.D. Becker, A.V. Balatsky, J.M. Wills, *J. Alloys Compd.* **287**, 1 (1999).
12. S.Y. Savrasov, G. Kotliar, *Phys. Rev. Lett.* **84**, 3670 (2000).
13. S.Y. Savrasov, G. Kotliar, E. Abrahams, *Nature (London)* **410**, 793 (2001).
14. J.M. Fournier, E. Pleska, J. Chiapusio, J. Rossat-Mignod, J. Rebizant, J.C. Spirlet, O. Vogt, *Physica B* **163**, 493 (1990).
15. K. Mattenberger, O. Vogt, *Physica Scripta T* **45**, 103 (1992).
16. M.S.S. Brooks, *J. Magn. Magn. Mat.* **63** & **64**, 649 (1987).
17. A. Hasegawa, H. Yamagami, *J. Magn. Magn. Mater.* **104-107**, 65 (1992).
18. P.M. Oppeneer, T. Kraft, M.S.S. Brooks, *Phys. Rev. B* **61**, 12825 (2000).
19. J. Schoenes, B. Frick, O. Vogt, *Phys. Rev. B* **30**, 6578 (1984).
20. P. Wachter, F. Marabelli, B. Bucher, *Phys. Rev. B* **43**, 11136 (1991).
21. O. Vogt, K. Mattenberger, in *Handbook on the Physics and Chemistry of Rare Earths*, edited by K.A. Gschneidner, Jr., L. Eyring, G.H. Lander, G.R. Choppin (North Holland, Amsterdam, 1993), p. 301.
22. G.H. Lander, A. Delapalme, P.J. Brown, J.C. Spirlet, J. Rebizant, O. Vogt, *Phys. Rev. Lett.* **53**, 2262 (1984).
23. G.H. Lander, *J. Magn. Magn. Mat.* **15-18**, 1208 (1980).
24. D.J. Lam, F.Y. Fradin, O.L. Kruger, *Phys. Rev.* **187**, 606 (1969).
25. O. Vogt, K. Mattenberger, J. Löhle, J. Rebizant, *J. All. Compds.* **271-273**, 508 (1998).
26. T. Gouder, F. Wastin, J. Rebizant, L. Havela, *Phys. Rev. Lett.* **48**, 3378 (2000).
27. A. Blaise, J.M. Collard, J.M. Fournier, J. Rebizant, J.C. Spirlet, O. Vogt, *Physica B* **130**, 99 (1985).
28. K. Mattenberger, O. Vogt, J.C. Spirlet, J. Rebizant, *J. Magn. Magn. Mat.* **54-57**, 539 (1986).
29. B.R. Cooper, R. Siemann, D. Yang, P. Thayamballi, A. Banerjee, in *Handbook on the Physics and Chemistry of the Actinides*, Vol. 2, edited by A.J. Freeman, G.H. Lander (North Holland, Amsterdam, 1985), p. 435.
30. A. Delin, L. Fast, B. Johansson, O. Eriksson, J.M. Wills, *Phys. Rev. B* **58**, 4345 (1998).
31. P. Strange, A. Svane, W.M. Temmerman, Z. Szotek, H. Winter, *Nature (London)* **399**, 756 (1999).
32. K.A. Gschneidner, *J. Less Common Metals*, **25**, 405, (1971).
33. A. Svane, W.M. Temmerman, L. Petit, Z. Szotek, unpublished.
34. L. Petit, A. Svane, W.M. Temmerman, Z. Szotek, *Phys. Rev. B* **63**, 165107 (2001).
35. O.K. Andersen, O. Jepsen, D. Glötzl, in *Canonical Description of the Band Structures of Metals, Proceedings of the International School of Physics, “Enrico Fermi”, Course LXXXIX, Varenna, 1985*, edited by F. Bassani, F. Fumi, M.P. Tosi (North-Holland, Amsterdam, 1985), p. 59.
36. B.L. Gyorffy, A.J. Pindor, J. Staunton, G.M. Stocks, H. Winter, *J. Phys. F* **15**, 1337 (1985).
37. L.J. Nugent, *J. Inorg. Nucl. Chem.* **32**, 3485 (1970).
38. B. Coqblin, J.R. Schrieffer, *Phys. Rev.* **185**, 847 (1969).
39. J.M. Wills, B.R. Cooper, *Phys. Rev. B* **42**, 4682 (1990).
40. K. Mattenberger, O. Vogt, J. Rebizant, J.C. Spirlet, F. Bourdarot, P. Burlet, J. Rossat-Mignod, M.N. Bouillet, A. Blaise, J.P. Sanchez, *J. Magn. Magn. Mat.* **104-107**, 43 (1992).
41. P. Villars, L.D. Calvert, *Pearson’s Handbook of Crystallographic Data for Intermetallic Phases*, Vols. 1+2, 2nd edn. (ASM International, Metals Park, OH, 1991).